BJP BRITISH JOURNAL OF PHARMACOLOGY

BPS BRITISH PHARMACOLOGICAL SOCIETY

British Journal of Pharmacology (2009), 158, 1895–1903

0007-1188/09
www.brjpharmacol.org

RESEARCH PAPER

U-shaped dose-dependent effects of BmK AS, a unique scorpion polypeptide toxin, on voltage-gated sodium channels

Mang-Mang Zhu[1,2]*, Jie Tao[2]*, Miao Tan[1], Hong-tian Yang[2] and Yong-Hua Ji[2]

[1]*School of Life Sciences, Shanghai University, Shanghai, China, and* [2]*Graduate School of Chinese Academy of Sciences, Shanghai Institute of Physiology, Shanghai Institute of Biological Sciences, Chinese Academy of Sciences, Shanghai, China*

Background and purpose: *Buthus martensi* Karsch (BmK) AS is a scorpion polypeptide toxin, said to target the voltage-gated sodium channels (VGSCs). However, the mechanism of action of BmK AS on the VGSCs has yet to be defined.
Experimental approach: We examined the electrophysiological effects of BmK AS in a wide dose range on the rat brain-type VGSC α-subunit, rNav1.2a, heterologously expressed in *Xenopus* oocytes and on the VGSCs endogenously expressed in the dorsal root ganglion neuroblastoma ND7-23 cell line.
Key results: In the oocytes, BmK AS depolarized the voltage dependence of activation and inactivation of rNav1.2a at 0.1 and 500 nM whereas these parameters were hyperpolarized at 1 nM. In ND7-23 cells, BmK AS hyperpolarized the voltage dependence of activation and inactivation at 0.1, 1 and 100 nM but not 10 nM. BmK AS also hyperpolarized the voltage dependence of recovery from inactivation at 0.1 and 100 nM and slowed the recovery kinetics at all concentrations, but the effects of 1 and 10 nM were relatively smaller than those at 0.1 and 100 nM. Moreover, the inactivation of VGSCs was potentiated by 10 nM BmK AS in both systems, whereas it was inhibited by 0.1 or 100 nM BmK AS in the oocytes or ND7-23 cells respectively.
Conclusions and implications: BmK AS modulated the VGSCs in a unique U-shaped dose-dependent manner, which could be due to the opposing effects of binding to two distinct receptor sites on the VGSCs.
British Journal of Pharmacology (2009) **158,** 1895–1903; doi:10.1111/j.1476-5381.2009.00471.x; published online 13 November 2009

Keywords: U-shaped dose-dependence; voltage-gated sodium channels; polypeptide modulator; scorpion toxin; electrophysiology

Abbreviations: AaH, *Androctonus australis* Hector; BmK, *Buthus martensi* Karsch; $[Ca^{2+}]_i$, intracellular calcium concentration; Css, *Centruroides suffusus suffusus*; Er_{Na}, reversal potential of sodium flow; I_{Na}, sodium current; I_{NaP}, persistent sodium current; I_{NaSS}, steady-state sodium current; I_{NaT}, transient sodium current; K_d, equilibrium dissociation constant; $[Na^+]_i$, intracellular sodium concentration; $V_{1/2}$, half-maximal voltage; VGSC, voltage-gated sodium channel

Introduction

The venom of the Asian scorpion *Buthus martensi* Karsch (BmK) is a rich source of biologically active peptides, with selective actions on a variety of ion channels. Over the past decade, 51 long-chain peptides have been isolated with action on voltage-gated sodium channels (VGSC). Among these, 34 are related to the α-toxin family, 4 related to the excitatory insect toxin family, 10 related to the depressant insect toxin family, 1 β-like toxin plus 2 unclassified polypeptides, BmK AS and AS-1 (Goudet *et al.*, 2002). BmK AS and AS-1 consist of 66 amino acids cross-linked by four disulphide bridges and their sequences exhibit 86.3% identity (Ji *et al.*, 1999). To date, no other natural toxin has been found to share sequence homology with them, except AaH IT4, an anti-insect toxin isolated from *Androctonus australis* Hector (AaH), active against the VGSCs (Loret *et al.*, 1991). An earlier study showed that BmK AS could significantly stimulate the binding of [^{3}H]-ryanodine to partially purified ryanodine receptors from rabbit skeletal muscle with an EC_{50} of 8 ± 1.6 μM, through an indirect mechanism (Kuniyasu *et al.*, 1999). Then BmK AS was found to promote noradrenaline release from rat hippocampus slices (0.05–1 mM) by augmentation of sodium influx (Ji *et al.*, 1997). Thus BmK AS

Correspondence: Dr Yong-Hua Ji, School of Life Sciences, Shanghai University, Shang-Da Road 99, Shanghai 200444, China. E-mail: yhji@staff.shu.edu.cn
*These two authors contributed equally to this work.
Correction added after online publication 30 November 2009: Author Mang-Mang Zhu's affiliations were amended to include School of Life Sciences and the affiliations were reordered.
Received 21 April 2009; revised 30 June 2009; accepted 12 July 2009

seems likely to enhance cell excitability through modulation of the VGSCs. However, later experiments on rat behaviour demonstrated that BmK AS could produce an anti-nociceptive effect on the inflammation-induced spontaneous pain as well as mechanical and thermal allodynia by intrathecal injection of 0.02–1.0 μg (Chen and Ji, 2002; Chen *et al*., 2006; Liu *et al*., 2008). Most recently, it was observed that hippocampal injection of 0.5–1 μg BmK AS repressed pentylenetetrazole-induced seizures in rat epilepsy models (R. Zhao and C.C. Weng, unpublished data). Electrophysiological recordings from neuroblastoma B104 cells showed that 50–500 nM of BmK AS could suppress VGSC currents by 15–25% (Tan *et al*., 2003). The reduction of VGSC currents was also observed without any effects on the voltage-dependent potassium and calcium currents in the acutely dissociated small dorsal root ganglion (DRG) neurons from rats in the presence of BmK AS at concentrations greater than 100 nM, leading to the suggestion that BmK AS could suppress neuronal excitability by inhibiting the sodium currents (I_{Na}) (Chen *et al*., 2006).

Little has been done to explain the differences in reported effects of BmK AS on cell excitability. Such differences might be attributed to the differential modulation by BmK AS of the various VGSC subtypes, or to the different doses used. To resolve these differences it is necessary to elucidate the mode of action of BmK AS before analysing the effects on the amplitude of I_{Na}. Moreover, binding assays indicated that the equilibrium dissociation constant (K_d) for BmK AS was ~0.46 nM on rat brain synaptosomes (Li *et al*., 2000), much lower than the concentrations tested in much of the earlier work.

In this study therefore, we investigated the modulating effects of BmK AS over a wide dose range from 0.05 to 500 nM on the rat brain-type VGSC α-subunit II [rNav1.2a; nomenclature follows Alexander *et al*. (2008)], heterologously expressed in *Xenopus* oocytes, as well as the VGSCs constitutively expressed in the DRG neuroblastoma ND7-23 cell line. The results showed BmK AS was distinguished from the other known polypeptide toxins by its unexpected, U-shaped dose-dependent effects on both brain-type and DRG-type VGSCs, although the detailed dose–response relationship differed in the two experimental systems.

Methods

cRNA preparation and expression

Plasmid pNa200 in combination with rNav1.2a cDNA was a gift from Dr Alan L Goldin (University of California, Irvine, CA, USA) and sequenced before RNA transcription. cRNAs of rNav1.2a were synthesized from Not I linearized DNA templates with T7 RNA polymerase message machine transcription kit (Ambion, Austin, TX, USA). The synthesized mRNA was analysed by agarose gel and reclaimed before storing in individual ampoules at –20°C.

Female *Xenopus laevis* frogs were provided by the animal centre of Shanghai Institute of Neuroscience. Oocytes were surgically removed and were incubated with collagenase (2 mg·mL^{-1}, type IA, Sigma, Saint Louis, MO, USA) in calcium-free OR_2 medium (in mM: 96 NaCl, 2 KCl, 1 $MgCl_2$ and 5 HEPES, pH 7.5) at 20°C for around 3 h. After washing, healthy oocytes at stage V–VI were selected for cRNA injection at a dose of 1–4 ng per oocyte and then incubated in ND96 medium (in mM: 96 NaCl, 2 KCl, 1.8 $CaCl_2$, 1 $MgCl_2$ and 5 HEPES, pH 7.5, supplemented with 5 pyruvate and 0.1 mg·mL^{-1} gentamicin) at 20°C for 40 h (Goldin, 1991).

Two-electrode voltage clamp recordings

Whole-cell currents were recorded at room temperature with TURBO TEC-03X amplifier (NPI Electronic Instruments, Tamm, Germany) and Cellworks E 5.5 software (NPI Electronic Instruments). The electrodes were filled with 3 M KCl and balanced in bath solution (ND96) for at least 30 min before recording. Data were sampled at 10 kHz and low-pass filtered at 1.3 kHz. Data acquisition was performed by Cellworks Reader 3.6 software (NPI Electronic Instruments). Capacitance transients and linear leakages were removed by subtracting the traces before and after 500 nM tetrodotoxin addition. Oocytes were not used when the leakages were beyond 0.10 μA.

Cell culture and whole-cell patch clamp recordings

ND7-23 cells (Shanghai cell bank of Chinese Academy of Science, Shanghai, China) were obtained from the Shanghai cell bank of the Chinese Academy of Science. The cells were cultured in Dulbecco's modified Eagle medium (DMEM; Gibco, Invitrogen, Grand Island, NY, USA) supplemented with 2 mM l-glutamine, 10% heat-inactivated fetal bovine serum (FBS; Gibco, Invitrogen). Culture dishes were incubated at 37°C in a humidified atmosphere containing 5% CO_2 and subcultured approximately every 2–3 days.

Whole-cell I_{Na} recordings were performed as described previously (John *et al*., 2004), using an EPC-9 amplifier (HEKA Elektronik, Lambrecht, Germany) at room temperature. Patch pipettes were fabricated from glass capillary tubes by PP-830 Puller (Narishige, Tokyo, Japan) with the resistance of 2–3 MΩ. The internal solution contained (in mM): 120 CsF, 10 HEPES, 10 EGTA, 15 NaCl, pH 7.25. The external solution contained (in mM): 140 NaCl, 5 HEPES, 1.3 $MgCl_2$, 1 $CaCl_2$, 11 glucose, 4.7 KCl, pH 7.4 (Sigma). The internal and external solutions were adjusted to osmolarities of 285–290 and 295–300 mOsm respectively.

Data acquisition and stimulation protocols were controlled by Pulse/PusleFit 8.3 software (HEKA Elektronik). Capacitance transients and series resistance errors were compensated by 75%. Cells were discarded when the series resistance values were over 20 MΩ. Linear leakage was subtracted using P/4 protocol. Data were sampled at 20 kHz and low-pass filtered at 10 kHz. The rate of solution exchange was studied using solutions with different NaCl concentrations and found to be about 95% complete within 60 s.

Electrophysiological protocols and data analysis

In *Xenopus* oocytes, the holding potentials were –100 mV. The I_{Na} were elicited by step pulses ranging from –100 to +65 mV for 100 ms with increments of 5 mV. The amplitudes of transient sodium currents (I_{NaT}) before and after BmK AS application were normalized to the peak I_{NaT} before BmK AS application to generate the *I–V* curves of the I_{NaT}. For deter-

mining the voltage dependence of activation, the sodium conductance was calculated using the formula:

$$G(V) = I(V)/(V - \mathrm{Er_{na}}) \quad (1)$$

where $I(V)$ is the I_{NaT} at the command voltage V, and $\mathrm{Er_{Na}}$ is the reversal potential of sodium flow estimated from the *I–V* curve. The conductances were normalized to the maximal value between –90 and +20 mV and fitted to a Boltzmann equation:

$$f(x) = -1/\{1 + \exp[(x - V_{1/2})/k]\} + 1 \quad (2)$$

where $V_{1/2}$ is the voltage at which half-maximal activation occurs, and k describes the slope of the fit. The inactivation kinetics was analysed by fitting the decay course of I_{NaT} to a tertiary exponential function:

$$f(t) = C + A_1 \exp[-(t - t_0)/\tau_1] + A_2 \exp[-(t - t_0)/\tau_2] + A_3 \exp[-(t - t_0)/\tau_3] \quad (3)$$

where t is time, t_0 is the time when the currents were just starting to exponentially decrease, A_1, A_2 and A_3 represent the amplitudes of channels inactivating with the time constants τ_1, τ_2 and τ_3, respectively, and C is the steady-state asymptote approximating to the non-inactivation persistent sodium current (I_{NaP}). The voltage dependence of fast and slow inactivation were analysed by two-pulse protocols, composed of a 10 or 100 ms prepulse, respectively, to potentials ranging from –100 to +30 mV with the increments of 10 mV followed by a test pulse of 0 mV for 50 ms. The amplitudes of the I_{Na} were normalized to their maximal value and plotted as channel availability versus prepulse potential. Data were then fitted to a Boltzmann equation:

$$f(x) = (1 - C)/\{1 + \exp[(x - V_{1/2})/k]\} + C \quad (4)$$

where $V_{1/2}$ is the voltage at which 50% of the fast- or slow-inactivation component is inactivated, k is the slope factor, and C is the steady-state asymptote.

The ND7-23 cells were held at the holding potential of –120 mV. I_{Na} were elicited by the step pulses ranging from –90 to +70 mV for 50 ms with increments of 5 mV. The voltage dependence of activation was analysed by the same procedure as in the *Xenopus* oocytes. The inactivation kinetics was analysed by fitting the decay course of I_{NaT} to a double exponential function:

$$f(t) = C + A_1 \exp[-(t - t_0)/\tau_1] + A_2 \exp[-(t - t_0)/\tau_2] \quad (5)$$

where t is time, t_0 is the time when the currents were just starting to exponentially decrease, A_1 and A_2 represent the amplitudes of the channels inactivating with the time constants τ_1 and τ_2, respectively, and C is the steady-state asymptote approximating to the leakage. Recovery kinetics were analysed by a traditional two-pulse protocol consisting of a 200 ms prepulse to 0 mV to inactivate all the VGSCs, followed by resting at –120 mV for the time in range of 1–39 ms with the increments of 2 ms, and a 10 ms test pulse to 0 mV. The current amplitude of the test pulse was divided by that of the prepulse, plotted as the recovery percentage versus the resting duration and fitted to a single exponential function:

$$f(t) = A[1 - \exp(-t/\tau)] \quad (6)$$

where t is time, A denotes the maximal recovery percentage with the time constant τ. The voltage dependence of recovery and fast inactivation was analysed by a multi-pulse protocol, composed of a 200 ms prepulse to 0 mV followed by a 5 ms rest at –120 mV to recover the fast component, a 3 ms prepulse to the potentials ranging from –150 to +30 mV with increments of 10 mV, and a 10 ms test pulse to 0 mV. The amplitudes of the I_{Na} were normalized to their maximal value and plotted versus the second prepulse potential. Data were then fitted to a double Boltzmann equation:

$$f(x) = f(1 - C)/\{1 - \exp[(x - V_{1/2\_1})/k_1]\} + (1 - f)(1 - C)/\{1 + \exp[(x - V_{1/2\_2})/k_2]\} + C \quad (7)$$

where f is the fraction of the recovery component, $V_{1/2\_1}$ and $V_{1/2\_2}$ are the voltages at which 50% of the channels are recovered and inactivated, respectively, k_1 and k_2 are the slope factors, and C is the steady-state asymptote. The voltage dependence of the slow inactivation was analysed by a traditional two-pulse protocol, composed of a 30 ms prepulse to potentials ranging from –150 to +30 mV with the increments of 10 mV followed by a 5 ms rest at –120 mV to recover the fast component, and a test pulse to 0 mV for 10 ms. The amplitudes of the I_{Na} were normalized to their maximal value, plotted versus the prepulse potential and then fitted to the Eqn 4.

The effects of BmK AS took about 5–10 min to appear and more than 30 min to achieve a stable effect (data not shown). In this study, unless indicated, the effects of each concentration of toxin were examined after perfusion for 20 min.

Data analysis

The raw data were analysed by Origin 8.0 (OriginLab, USA). The results are shown as means ± SEM with the number of experiments shown as n in the figure legends. Differences between means were analysed by Student's test or by one-way ANOVA, with $P < 0.05$ taken to show a significant difference.

Materials

The crude BmK venom was purchased from a scorpion culture farm in He-Nan Province, China. The venom was filtered with a Sephadex G-50 column and purified as described by Liu *et al.* (1996). The purity of the toxin was confirmed by mass spectrometry as well as peptide sequencing. Stock solutions of BmK AS (0.1 mM BmK AS plus 25 g·L^{-1} BSA) was dissolved in the bath solution to yield the desired concentration before the electrophysiological recording.

Results

U-shaped dose-dependent shift of the voltage dependence of activation

The effects of 0.1, 1, 10, 100 and 500 nM of BmK AS were determined on the rNav1.2a subunits expressed heterologously in *Xenopus* oocytes. The I_{Na} of rNav1.2a were evoked by 100 ms step pulses ranging from –100 to +65 mV (Figure 1A–

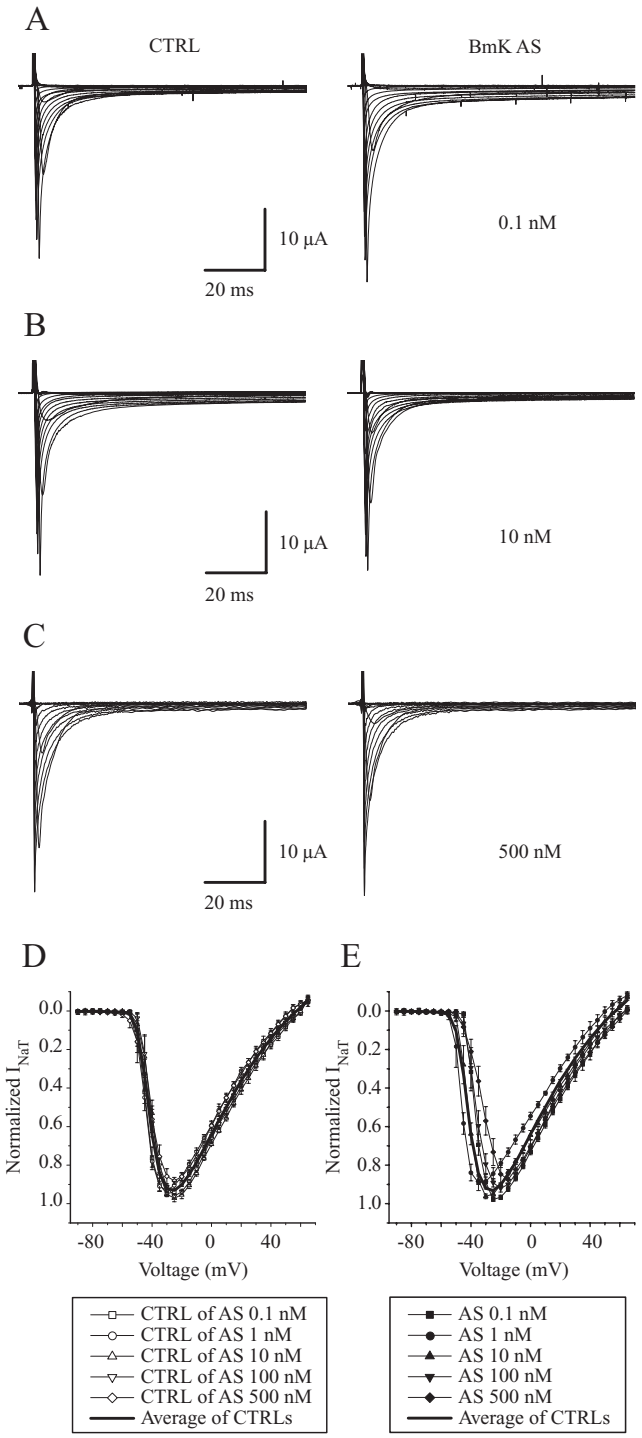

Figure 1 Effect of BmK AS on the *I–V* relationship of rNav1.2a. The sodium currents were evoked by step pulses ranging from –100 to +65 mV for 100 ms from the holding potential of –100 mV in increments of 5 mV. (A–C) Representative sodium currents before and after application of 0.1, 10 or 500 nM BmK AS, shown at intervals of 10 mV. (D–E) Statistical plots of the *I–V* relationship of rNav1.2a before (D) and after (E) application of 0.1, 1, 10, 100 and 500 nM BmK AS. Each oocyte was subjected to one concentration of BmK AS for 20 min. n = 12, 10, 10, 10 and 14 respectively. BmK, *Buthus martensi* Karsch; I_{NaT}, transient sodium current.

C). Before application of BmK AS, the samples were selected if they were provided with accordant *I–V* relationship of the I_{NaT} with the peak I_{NaT} appearing at voltages between –30 and –20 mV (Figure 1D). After perfusion with 500 nM BmK AS for 20 min, the *I–V* curve of the I_{NaT} was shifted in a depolarized direction (Figure 1E). A similar but not significant effect could be observed in the presence of 0.1 nM BmK AS, whereas 1 nM BmK AS imposed a slight opposite effect (Figure 1E). Taking into consideration the changes in the Er_{Na}, the voltage dependence of activation was then analysed by fitting the conductance–voltage (*G–V*) relationship of the I_{NaT} to a Boltzmann function (see *Methods*). As a result, only the highest concentration of BmK AS (500 nM) significantly moved the half-maximal voltage ($V_{1/2}$) of activation (Table 1) towards depolarization by 10.3 mV, compared with the control value, before BmK AS application. However, the $V_{1/2}$ values for both 0.1 and 500 nM BmK AS were significantly different from each other.

In the DRG neuroblastoma ND7-23 cells, the I_{Na} were activated by 50 ms step pulses in the range from –90 to +70 mV (Figure 2A,B), and they shared a homogenous *I–V* relationship and always peaked at voltages between –10 and 0 mV in the absence of BmK AS. After perfusion with 0.1, 1 or 100 nM BmK AS, the *I–V* curve was significantly hyperpolarized (Figure 2C) with decreased $V_{1/2}$ of activation (Table 2). However at 10 nM, BmK AS did not affect the *I–V* curve or the $V_{1/2}$ of activation (Figure 2D and Table 2). As the effects of 0.1 and 100 nM BmK AS were large, we measured the effects at intermediate concentrations (0.05 and 30 nM). The results (Figure S1A) showed that these concentrations exerted correspondingly intermediate effects shifting the $V_{1/2}$ of activation by –6.0 (0.05 nM) and –9.2 mV (30 nM). Thus, the voltage dependence of activation of ND7-23 VGSCs was also modulated by BmK AS in a U-shaped dose-dependent manner, as in oocytes expressing rNav1.2a.

U-shaped dose-dependent shift of the voltage dependence of inactivation

When expressed in *Xenopus* oocytes, a proportion of the fast-gating rNav1.2a channels take on the character of the slow-gating VGSCs and inactivate in a process called slow inactivation, which is mechanistically different from fast inactivation. We could therefore analyse the effects of the toxin on the voltage dependence of fast and slow inactivation, separately. As shown in Table 1, the $V_{1/2}$ of either fast or slow inactivation was shifted to less negative values (depolarization) by 0.1 and 500 nM BmK AS. No changes in the inactivation process were induced by the other concentrations of BmK AS (10 and 100 nM)

In the ND7-23 cells, the endogenous VGSCs inactivate rapidly and completely. However, they consisted of two components inactivating with different time constants (see below), and the slower inactivation was more affected by BmK AS than the faster inactivation (Figure 3). In terms of the $V_{1/2}$ of inactivation (Table 2), the fast inactivation was not changed over the concentration range used (0.1–100 nM), but the slow inactivation process was shifted to more negative values at 0.1 and 100 nM BmK AS.

It is relevant here to note that the slope factor (k) of the fast inactivation curve of both rNav1.2a (Table 1) and the ND7-23

Table 1 Parameters for voltage dependence of activation and inactivation of rNav1.2a expressed in *Xenopus laevis* oocytes

Concentration	*CTRL*	*0.1 nM*	*1 nM*	*10 nM*	*100 nM*	*500 nM*
n	*56*	*12*	*10*	*10*	*10*	*14*
Activation						
$V_{1/2}$ (mV)	−40.9 ± 0.19	−36.0 ± 0.26#	−45.4 ± 0.15	−41.2 ± 0.16	−37.1 ± 0.24#	−30.8 ± 0.22*#
k (mV)	4.2 ± 0.16	3.6 ± 0.23	3.0 ± 0.13	3.5 ± 0.14	4.4 ± 0.21	5.6 ± 0.19
Fast inactivation						
$V_{1/2}$ (mV)	−42.0 ± 0.87	−36.7 ± 0.64#	−46.8 ± 0.74	−40.9 ± 1.02	−41.2 ± 1.17	−33.3 ± 0.97*#
k (mV)	5.6 ± 0.65	5.9 ± 0.48	6.4 ± 0.56	6.0 ± 0.76	5.8 ± 0.91	8.4 ± 0.74*
Slow inactivation						
$V_{1/2}$ (mV)	−51.9 ± 0.58	−41.7 ± 0.37*#	−55.6 ± 0.46	−51.6 ± 0.94	−51.1 ± 0.54	−38.2 ± 0.66*#
k (mV)	5.4 ± 0.43	5.7 ± 0.26	5.6 ± 0.35	5.3 ± 0.52	5.4 ± 0.24	6.9 ± 0.41

*P < 0.05; significant difference between control and *Buthus martensi* Karsch (BmK) AS values; one-way ANOVA.
#P < 0.05; significant difference between BmK AS at 1 nM and the other concentrations; one-way ANOVA.

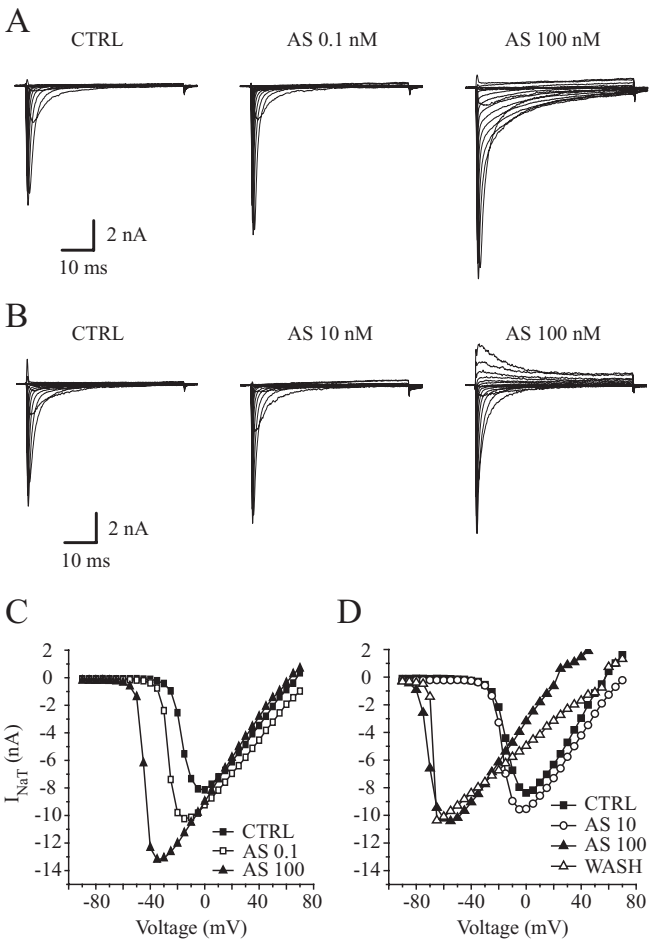

Figure 2 Effect of BmK AS on the *I–V* relationship of the VGSCs in ND7-23cells. The sodium currents were evoked by step pulses ranging from −90 to +70 mV for 50 ms from the holding potential of −120 mV in increments of 5 mV. (A–B) Representative sodium currents before and after perfusion for 20 min with 0.1 and 100 nM (A), or 10 and 100 nM (B) BmK AS in succession, shown at intervals of 10 mV. (C–D) *I–V* relationship of the representative sodium currents shown in (A) and (B), respectively. Note that in (D), the Er_{Na} decreased after application of 100 nM BmK AS and recovered after washing, indicating that the change of the Er_{Na} was caused by the toxin, not by membrane leakage. BmK, *Buthus martensi* Karsch; Er_{Na}, reversal potential of sodium flow; I_{NaT}, transient sodium current; VGSC, voltage-gated sodium channel.

VGSCs (Table 2) was increased by the higher concentrations of BmK AS (500 or 100 nM respectively)

Bidirectional effects on the open-state inactivation kinetics

The slowly inactivating rNav1.2a subunits produced steady-state sodium currents (I_{NaSS}) present at the end of the 100 ms depolarizing pulses in *Xenopus* oocytes. BmK AS enhanced the I_{NaSS} at 0.1 nM (Figure 1A) but reduced it at 10 nM (Figure 1B; mean values in Figure 4A). Kinetic analysis of the inactivation showed that BmK AS did not affect the inactivation time constants (Figure 4B) but did change the ratio between the fast- and the slow-inactivation components. In the presence of 0.1 nM BmK AS, a small but significant fraction of the VGSCs were transformed from the fast-inactivation component into the slow-inactivation component, whereas in the presence of 10 nM of BmK AS, an equal fraction of VGSCs were transformed from the slow-inactivation component into the fast-inactivation component (Figure 4C).

Likewise, the inactivation kinetics of the ND7-23 VGSCs was affected by BmK AS in a bidirectional manner. In the absence of BmK AS, after depolarization to +10 mV for 10 ms, there was only about 2% of the I_{Na} left. This residual current was reduced by about 40% by 10 nM, whereas it was enhanced several fold by 100 nM BmK AS (Figure 4D). The acceleration of the inactivation with 10 nM BmK AS was not only due to the slight decrease of the fast-inactivation time constant (Figure 4E) but also to the increased proportion of the faster component (Figure 4F). Meanwhile, the deceleration of the inactivation with 100 nM BmK AS could be attributed partly to the increase of the slow-inactivation time constant (Figure 4E) and partly to the increased proportion of the slower component (Figure 4F). Nevertheless, 10 nM BmK AS also increased the slower inactivation time constant (Figure 4E), and the effect was not significantly different (P = 0.89, one-way ANOVA) from that of 100 nM BmK AS.

U-shaped dose-dependent inhibition of the recovery from inactivation

For kinetic correlations between the inactivation and recovery from inactivation of VGSC, recovery kinetics were examined on the ND7-23 VGSCs. As shown in Figure 5, the time course of recovery within 39 ms was fitted well with a single expo-

Table 2 Parameters for voltage dependence of activation, inactivation and recovery of the ND7-23 VGSCs

Concentration	*CTRL*	*0.1 nM*	*1 nM*	*10 nM*	*100 nM*
n	*46*	*12*	*10*	*12*	*12*
Activation					
$V_{1/2}$ (mV)	−21.8 ± 0.23	−31.3 ± 0.46*	−30.0 ± 0.54*	−25.5 ± 0.97	−39.9 ± 0.61*
k (mV)	7.7 ± 0.28	7.0 ± 0.35	6.7 ± 0.41	6.1 ± 0.53	9.5 ± 0.56
Fast inactivation					
$V_{1/2}$ (mV)	−24.0 ± 0.34	−31.7 ± 0.38	−28.7 ± 0.29	−25.5 ± 0.48	−31.8 ± 1.15
k (mV)	8.2 ± 0.27	9.3 ± 0.28	9.3 ± 0.22	8.3 ± 0.38	14.0 ± 0.77*
Slow inactivation					
$V_{1/2}$ (mV)	−42.1 ± 0.95	−57.0 ± 0.59*	−48.6 ± 0.87	−41.0 ± 1.22	−76.9 ± 0.56*
k (mV)	10.8 ± 0.54	12.5 ± 0.38	12.3 ± 0.33	11.8 ± 0.49	13.0 ± 0.26
Recovery					
$V_{1/2}$ (mV)	−98.1 ± 4.04	−110.0 ± 0.89*	−101.1 ± 1.10	−103.8 ± 2.22	−109.0 ± 1.02*
k (mV)	10.8 ± 3.38	12.9 ± 0.99	10.9 ± 0.92	11.0 ± 2.06	9.7 ± 0.95

*$P < 0.05$; significant difference between control and BmK AS; one-way ANOVA.
BmK, *Buthus martensi* Karsch; VGSC, voltage-gated sodium channel.

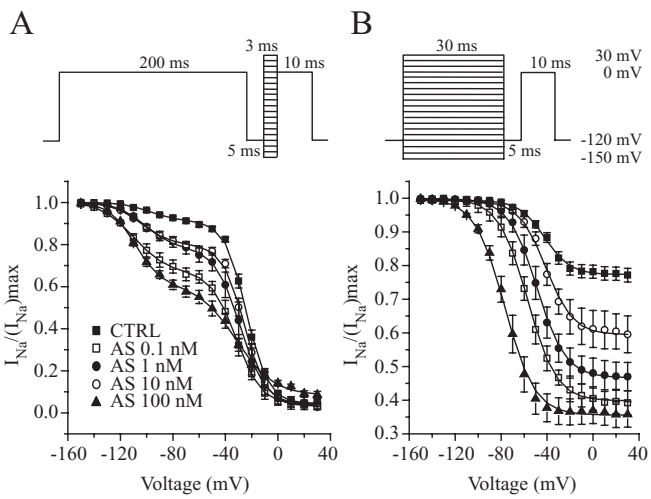

Figure 3 Effects of BmK AS on the voltage dependence of inactivation and recovery from inactivation in ND7-23 cells. Each cell was subjected to one concentration of BmK AS. $n = 46$, 12, 10, 12 and 12, respectively, in control and BmK AS of 0.1, 1, 10 and 100 nM. (A) Voltage dependence of the recovery and the faster inactivation, analysed by a multi-pulse protocol (top) composed of a 200 ms prepulse to 0 mV followed by 5 ms resting at −120 mV to recover the fast component, a 3 ms prepulse to the potentials ranging from −150 to +30 mV in increments of 10 mV, and a 10 ms test pulse to 0 mV. The plots of channel availability versus voltage of the second prepulse (below) fitted well with a double Boltzmann function, where the first phase represents the voltage-dependent decrease of recovery and the second phase represents the voltage-dependent increase of inactivation. The fitting parameters are indicated in Table 2. (B) Voltage dependence of the slow inactivation, analysed by a classical two-pulse protocol (top) composed of a 30 ms prepulse to potentials ranging from −150 to +30 mV in increments of 10 mV followed by 5 ms resting at −120 mV to recover the faster component, and a test pulse to 0 mV for 10 ms. The plots of channel availability versus prepulse voltage (below) fitted well to a single Boltzmann function and the fitting parameters are indicated in Table 2. BmK, *Buthus martensi* Karsch; I_{Na}, sodium current.

nential function before and after application of BmK AS, and the recovery time constant was increased by BmK AS from 3.22 ± 0.18 ms to 8.34 ± 0.19, 8.20 ± 0.21, 5.94 ± 0.19 and 11.9 ± 0.31 ms, at the concentration of 0.1, 1, 10 and 100 nM respectively (Figure 5). Moreover, 0.1 and 100 nM BmK AS shifted the voltage dependence of recovery significantly towards hyperpolarization (Figure 3A and Table 2), leading to the decline of the total recovery of the VGSCs at −120 mV shown in Figure 5, whereas 1 and 10 nM BmK AS did not alter total recovery. In addition, 0.05 and 30 nM BmK AS also showed intermediate effects for recovery, compared with the effects of 0.1 and 100 nM BmK AS (Figure S1B). Overall our results showed that, in ND7-23 cells, BmK AS inhibited the recovery of VGSCs from the inactivation in a U-shaped, dose-dependent manner.

Bidirectional modulation of the I_{Na} amplitude at different concentration

Alteration of the amplitude of the I_{Na} represents the complex effects of the toxin. In the presence of 0.1 nM BmK AS, the peak I_{NaT} of rNav1.2a (Figure 6A) and ND7-23 cells (Figure 6B) was enhanced by 14.9 ± 1.3% and 33.7 ± 4.7% respectively. At the highest concentration used in ND7-23 cells (300 nM BmK AS), around 90% of the I_{Na} was blocked (Figure 6B and Figure S2), but no significant effects were detected with the other concentrations of BmK AS. Thus BmK AS increased I_{Na} at a low concentration and reduced I_{Na} at high concentrations.

Discussion

From our results, we concluded that BmK AS (0.1–500 nM) modulated the activation, inactivation and recovery of the brain and DRG-type VGSCs in a U-shaped dose-dependent manner. This U-shaped dose-dependence is a unique feature of BmK AS among the polypeptide modulators of VGSC, acting extracellularly. Such U-shaped curves are more usually found with synthetic, small molecules, bearing two or more binding sites, responsible for opposite effects. In the *Xenopus* oocytes, BmK AS had both depolarizing and hyperpolarizing effects on the voltage dependence of activation and inactivation of rNav1.2a. BmK AS also exerts its enhancing effects at the same time as its inhibitory effects, on the open-state VGSC inactivation in both systems. Hence, the U-shaped character of the response curve for BmK AS might be

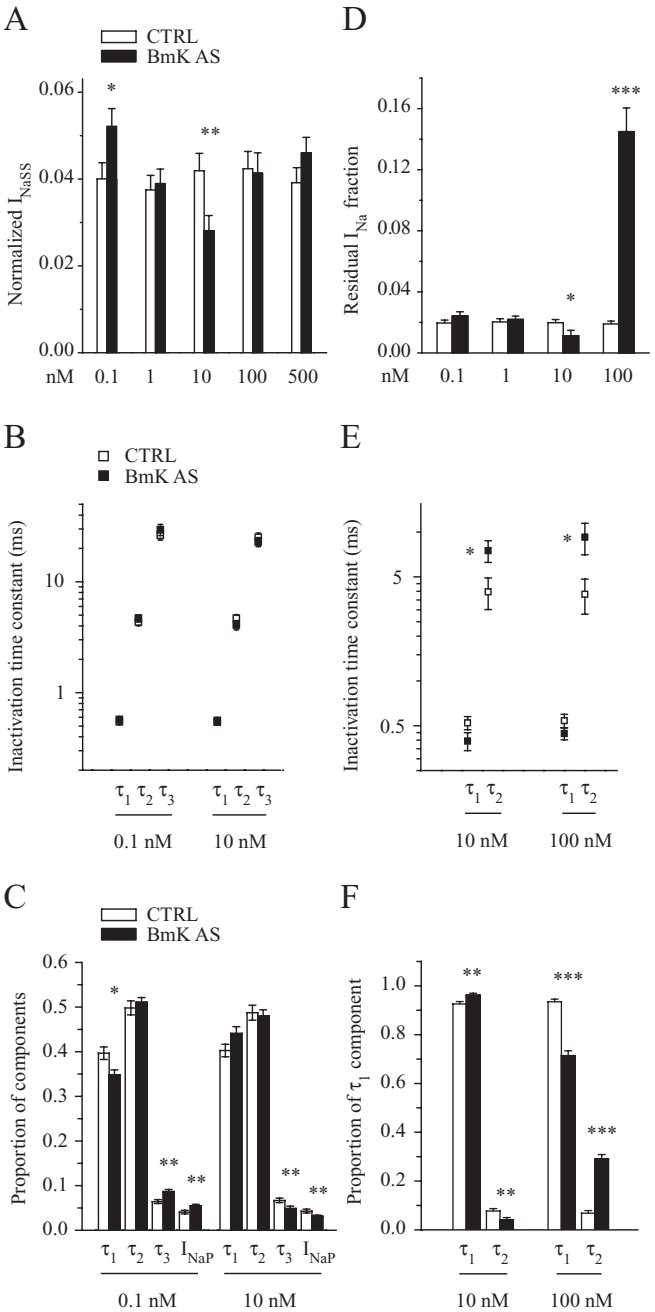

Figure 4 Effects of BmK AS on the inactivation kinetics. (A) The proportion of steady-state rNav1.2a current at the end of depolarization for 100 ms to –20 mV, before and after application of 0.1, 1, 10, 100 or 500 nM BmK AS for 20 min. n = 12, 10, 10, 10 and 14 respectively. The I_{NaSS} was measured as the mean of the remainder currents during 99–100 ms. (B,C) Kinetic analysis of the inactivation of rNav1.2a at –20 mV in the absence and presence of 0.1 (n = 8) or 10 (n = 8) nM BmK AS. The decay time course of the sodium currents at –20 mV were fitted with a ternary exponential function, by which two fast-inactivation components (τ_1 and τ_2) and two slow-inactivation components (τ_3 and I_{NaP}) were separated according to the inactivation time constant (B). (C) The proportion of four inactivation components of rNav1.2a at –20 mV. (D) The fraction of residual sodium current after depolarization to +10 mV for 10 ms in ND7-23 cells, before and after application of 0.1, 1, 10 or 100 nM BmK AS for 20 min. n = 12, 10, 12 and 12 respectively. (E,F) Kinetic analysis of the inactivation of ND7-23 VGSCs at +10 mV in the absence and presence of 10 (n = 7) or 100 (n = 7) nM BmK AS. The decay time course of the sodium currents at +10 mV were fitted with a double exponential functions, by which a faster-(τ_1) inactivation component and a slowish-inactivation component (τ_2) were separated according to the inactivation time constant (E). (F) The proportion of two inactivation components of the ND7-23 VGSCs at +10 mV. *P < 0.05, **P < 0.01 and ***P < 0.001; significant difference between the control and BmK AS values; paired Student's t-test. BmK, *Buthus martensi* Karsch; I_{Na}, sodium current; I_{NaP}, persistent sodium current; I_{NaSS}, steady-state sodium current; VGSC, voltage-gated sodium channel.

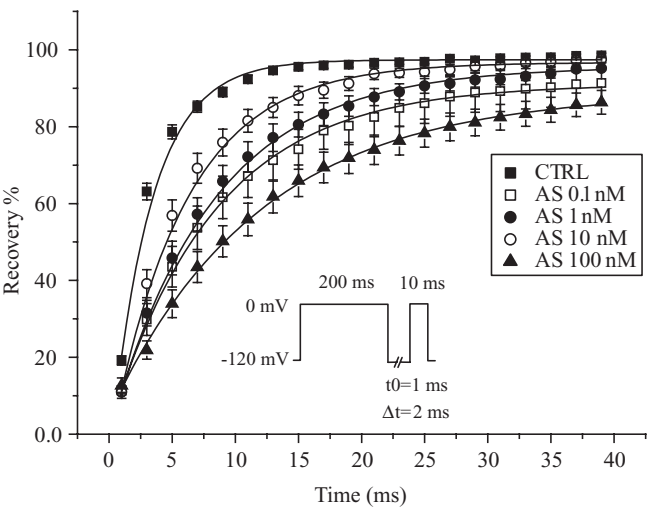

Figure 5 Effect of *Buthus martensi* Karsch (BmK) AS on the recovery from inactivation in ND7-23 cells. The time course of recovery at –120 mV was determined by a two-pulse protocol (inset), consisting of a 200 ms prepulse to 0 mV followed by resting at –120 mV for the time varying from 1 to 39 ms in increments of 2 ms, and a test pulse to 0 mV for 10 ms. The recovery time course was then fitted with a single exponential function to obtain the time constant of recovery. Before application of BmK AS (CTRL), the recovery time constant was 3.22 ± 0.18 ms (n = 36). After application of 0.1, 1, 10 or 100 nM BmK AS, it increased to 8.34 ± 0.19 (n = 9), 8.20 ± 0.21 (n = 9), 5.94 ± 0.19 (n = 9) or 11.9 ± 0.31 (n = 9) ms respectively. All the concentrations of BmK AS increased the recovery time constant significantly (P < 0.05). Also the effects of 0.1 and 100 nM were significantly different from the effect of 10 nM (P < 0.05); one-way ANOVA.

explained by its occupation of two different receptor sites, one of which is of higher affinity and responsible for the inhibition of inactivation, whereas the other is of lower affinity and responsible for the potentiation of inactivation. Binding of BmK AS to two such sites would also result in the shift of the voltage in opposite directions. The relative strength of the opposing effects would depend on the toxin concentration and the VGSC subtype.

Among the scorpion polypeptide toxins targeting the VGSCs, inhibition of the inactivation and recovery is the distinctive characteristic of the α-toxins, exerted via the receptor site-3, while a negative shift of the voltage dependence of activation is characteristic for the β-toxins, via the receptor site-4. Our results indicate that BmK AS exhibits the pharmacological activities of both the α- and β-toxins. This finding is in accord with earlier results showing that BmK AS-1 and AaH IT4 were both recognized by the anti-β-toxin antibodies (Loret *et al.*, 1991; Jia *et al.*, 2000) and compete

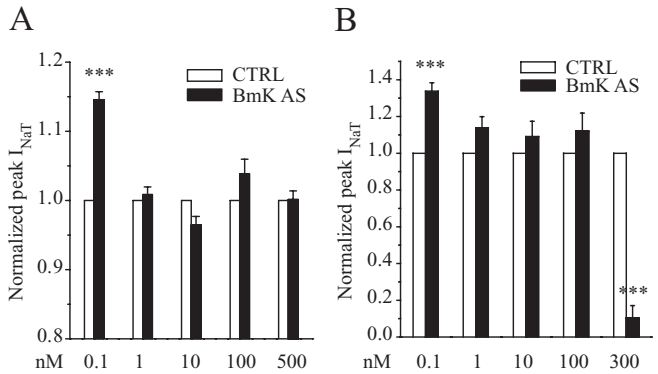

Figure 6 Effect of *Buthus martensi* Karsch (BmK) AS on the amplitudes of sodium currents. (A) The normalized value of peak transient sodium current (I_{NaT}) of rNav1.2a expressed in *Xenopus* oocytes in the presence of 0.1, 1, 10, 100 and 500 nM BmK AS. n = 12, 10, 10, 10 and 14 respectively. (B) The normalized value of peak I_{NaT} in ND7-23 cells in the presence of 0.1, 1, 10, 100 and 300 nM BmK AS. n = 12, 10, 12, 12 and 7 respectively. ***P < 0.001 significant difference between the control and BmK AS; paired Student's t-test.

with both the α- and β-toxins for binding to the VGSCs (Loret *et al.*, 1991; Jia *et al.*, 1999). On the other hand, Css IV, a typical β-toxin from the American scorpion *Centruroides suffusus suffuses* (Css) bound to the rat brain VGSCs at two types of specific high-affinity sites: a variable minor type with K_d of ~0.1 nM and a major type with a K_d of ~5 nM (Thomsen *et al.*, 1995). Because our results also implied two classes of binding sites with affinities around 0.1 and 10 nM BmK AS on the rat brain- and DRG-type VGSCs, the binding sites for BmK AS and Css IV might be analogous or overlapping, and the variable minor sites for Css IV might become the major sites for BmK AS to exert a α-toxin-like modulation. However, BmK AS did facilitate activation without the depolarizing pre-stimulation that is required for Css IV (Cestele *et al.*, 1998), suggesting the binding sites for BmK AS to exert its β-toxin-like modulation must be different from that for Css IV.

The effect of the charge of the polypeptide may be important at high concentration of BmK AS. Although the higher concentrations used here were still sub-micromolar, the positive charges in BmK AS may affect the surface potential of the cell membrane near the VGSC and thus change the VGSC microenvironment. In the presence of high concentrations of BmK AS, such a charge effect may become dominant, inducing hyperpolarization of the voltage dependence of these channels, as well as the Er_{Na} (Figure 2D). Nevertheless, any charge effect of BmK AS could not exclude the possibility that the polypeptide AS binds to site-4, as BmK AS facilitated activation before inducing the shift of Er_{Na} (Figure S3).

A marked reduction of the I_{Na} can block the firing of action potentials, and this has been suggested to be the mechanism of BmK AS in inducing analgesic effects (Chen *et al.*, 2006). The amplitude of I_{Na} is influenced by many factors including the amount of available channels, the single channel conductance, the voltage dependence, kinetics and the concentration of intracellular and extracellular sodium ions. In this study, we found that BmK AS increased the I_{Na} at an extremely low concentration of 0.1 nM in both systems. We expected this effect to be U-shaped dose-dependent. However, high concentrations of BmK AS reduced the I_{Na} in ND7-23 cells, as in the acutely dissociated DRG neurons. This may be due partly to the marked negative shift of the Er_{Na} reducing the driving force of sodium influx. At the same time it seems that the strong hyperpolarizing shift of the voltage dependence of inactivation (Figure 3) contributed more to the abolition of the I_{Na} by high dose of BmK AS. As shown in Figure S2, the I_{Na} was abolished by 300 nM BmK AS when the holding potential was –120 mV, but some of the I_{Na} recovered when the holding potential was changed to –160 mV, demonstrating that inactivation of the closed-state VGSCs is an important component of the action of BmK AS on the DRG-type VGSCs. Higher concentrations of BmK AS no longer increased the I_{Na} amplitude in *Xenopus* oocytes expressing rNav1.2a. This may be because the voltage dependence of activation of rNav1.2a was more shifted than the Er_{Na} in a depolarizing direction by 500 nM BmK AS, thus reducing the driving force of sodium influx.

Although high concentrations of BmK AS severely reduced the I_{Na} via hyperpolarizing the voltage dependence of DRG neuroblastoma VGSCs, the polypeptide may simultaneously activate I_{Na} near the resting potential, which might result in a raised intracellular sodium concentration ($[Na^+]_i$). In the neuroblastoma B104 cells, 500 nM BmK AS elevated the $[Na^+]_i$ by 18% at the resting potential (Tan *et al.*, 2004). Increased $[Na^+]_i$ can induce increased intracellular calcium concentration ($[Ca^{2+}]_i$), which in turn activates downstream signalling pathways affecting ion channels and transporters. Thus, the effect of BmK AS on cell excitability are not only regulated by the concentration of BmK AS, but are also dependent upon the expression of various proteins within different cell types that functionally influence the $[Na^+]_i$ and $[Ca^{2+}]_i$.

Acknowledgements

We are grateful to Dr Alan L Goldin (University of California, USA) for kind provision of the plasmid pNa200. We also thank Dr Wolfgang Schwarz (Max-Planck Institute, Germany) for his help in setting up the *X. laevis* oocyte expression system and two-electrode voltage clamp recording system. This study was supported by National Basic Research Program of China (2006CB500801), and partially by National Nature Sciences Foundation of China (30270428) and Science and Technology Commission of Shanghai Municipality (08JC1409500).

Conflict of interest

The authors state no conflict of interest.

References

Alexander SP, Mathie A, Peters JA (2008). Guide to receptors and channels (GRAC), 3rd edition. *Br J Pharmacol* **153** (Suppl. 2): S1–S209.

Cestele S, Qu Y, Rogers JC, Rochat H, Scheuer T, Catterall WA (1998). Voltage sensor-trapping: enhanced activation of sodium channels

by beta-scorpion toxin bound to the S3-S4 loop in domain II. *Neuron* **21**: 919–931.
Chen B, Ji Y (2002). Antihyperalgesia effect of BmK AS, a scorpion toxin, in rat by intraplantar injection. *Brain Res* **952**: 322–326.
Chen J, Feng XH, Shi J, Tan ZY, Bai ZT, Liu T *et al*. (2006). The anti-nociceptive effect of BmK AS, a scorpion active polypeptide, and the possible mechanism on specifically modulating voltage-gated Na^+ currents in primary afferent neurons. *Peptides* **27**: 2182–2192.
Goldin AL (1991). Expression of ion channels by injection of mRNA into *Xenopus* oocytes. *Methods Cell Biol* **36**: 487–509.
Goudet C, Chi CW, Tytgat J (2002). An overview of toxins and genes from the venom of the Asian scorpion *Buthus martensi* Karsch. *Toxicon* **40**: 1239–1258.
Ji YH, Huang HY, Zhang JW, Hoshino M, Mochizuki T, Yanaihara N (1997). BmK AS, an active scorpion polypeptide, enhances [^{3}H]-noradrenaline release from rat hippocampal slices. *Biomed Res* **18**: 257–260.
Ji YH, Li YJ, Zhang JW, Song BL, Yamaki T, Mochizuki T *et al*. (1999). Covalent structures of BmK AS and BmK AS-1, two novel bioactive polypeptides purified from Chinese scorpion *Buthus martensi* Karsch. *Toxicon* **37**: 519–536.
Jia LY, Zhang JW, Ji YH (1999). Biosensor binding assay of BmK AS-1, a novel Na^+ channel-blocking scorpion ligand on rat brain synaptosomes. *Neuroreport* **10**: 3359–3362.
Jia LY, Xie HF, Ji YH (2000). Characterization of four distinct monoclonal antibodies specific to BmK AS-1, a novel scorpion bioactive polypeptide. *Toxicon* **38**: 605–617.
John VH, Main MJ, Powell AJ, Gladwell ZM, Hick C, Sidhu HS *et al*. (2004). Heterologous expression and functional analysis of rat Nav1.8 (SNS) voltage-gated sodium channels in the dorsal root ganglion neuroblastoma cell line ND7-23. *Neuropharmacology* **46**: 425–438.
Kuniyasu A, Kawano S, Hirayama Y, Ji YH, Xu K, Ohkura M *et al*. (1999). A new scorpion toxin (BmK-PL) stimulates Ca^{2+}-release channel activity of the skeletal-muscle ryanodine receptor by an indirect mechanism. *Biochem J* **339** (Pt 2): 343–350.
Li YJ, Liu Y, Ji YH (2000). BmK AS: new scorpion neurotoxin binds to distinct receptor sites of mammal and insect voltage-gated sodium channels. *J Neurosci Res* **61**: 541–548.
Liu T, Pang XY, Jiang F, Bai ZT, Ji YH (2008). Anti-nociceptive effects induced by intrathecal injection of BmK AS, a polypeptide from the venom of Chinese-scorpion *Buthus martensi* Karsch, in rat formalin test. *J Ethnopharmacol* **117**: 332–338.
Liu Y, Ren HM, Ji YH, Ohishi T, Mochizuki T, Hoahino M *et al*. (1996). Purification and the partial amino acid sequence of a novel activator of Ryanodine (BmK AS-1) from mammalian skeletal muscle. *Biomed Res* **17**: 451–455.
Loret EP, Martin-Eauclaire MF, Mansuelle P, Sampieri F, Granier C, Rochat H (1991). An anti-insect toxin purified from the scorpion *Androctonus australis* Hector also acts on the alpha- and beta-sites of the mammalian sodium channel: sequence and circular dichroism study. *Biochemistry* **30**: 633–640.
Tan ZY, Chen J, Shun HY, Feng XH, Ji YH (2003). Modulation of BmK AS, a scorpion neurotoxic polypeptide, on voltage-gated Na^+ channels in B104 neuronal cell line. *Neurosci Lett* **340**: 123–126.
Tan ZY, Chen J, Feng XH, Susumu T, Ji YH (2004). Modulation of intracellular Na^+ concentration by BmK AS, a scorpion toxin, in B104 cell line. *Neuroreport* **15**: 13–16.
Thomsen W, Martin-Eauclaire MF, Rochat H, Catterall WA (1995). Reconstitution of high-affinity binding of a beta-scorpion toxin to neurotoxin receptor site 4 on purified sodium channels. *J Neurochem* **65**: 1358–1364.

Supporting Information

Additional Supporting Information may be found in the online version of this article:

Figure S1 Effect of 0.05 nM ($n = 8$) and 30 nM ($n = 8$) *Buthus martensi* Karsch (BmK) AS on the activation (A) and recovery (B) of the ND7-23 voltage-gated sodium channels (VGSCs), analysed as described in *Methods*. The fitting parameters ($V_{1/2}$ and k) of activation and the time constant of recovery are indicated as follows: –20.3 ± 0.37 mV, 8.0 ± 0.25 mV, 3.44 ± 0.22 ms (CTRL); –26.3 ± 0.13 mV, 7.3 ± 0.08 mV, 6.48 ± 0.22 ms (0.05 nM); –29.5 ± 0.26 mV, 8.6 ± 0.19 mV, 7.56 ± 0.12 ms (30 nM). 10 nM ($n = 4$, 6.08 ± 0.13 ms) and 100 nM ($n = 4$, 9.97 ± 0.27 ms) BmK AS were used for two positive controls to make sure the consistency of the toxin efficiency of BmK AS.
Figure S2 (A–C) Raw sodium currents before (A) and after (B and C) application of 300 nM *Buthus martensi* Karsch (BmK) AS for 20 min in ND7-23 cells. The currents were activated by step pulses ranging from –90 to +70 mV with the increments of 5 mV from the holding potential of –120 mV (A and B) or –160 mV (C). (D) *I–V* relationship of the currents in (A–C). Note the I_{Na} was completely abolished by 300 nM BmK AS when holding potential was –120 mV, but some of it recovered when holding potential was changed to –160 mV.
Figure S3 Representative example of the two-phase impact of 100 nM *Buthus martensi* Karsch (BmK) AS. At the first phase, the toxin only shifts the voltage dependence without changing the reversal potential of sodium flow (Er_{Na}). At the second phase however, the toxin severely shifts the Er_{Na} with further hyperpolarization of the voltage dependence. Note the time for BmK AS shifting the Er_{Na} is variable among the cells.

Please note: Wiley-Blackwell are not responsible for the content or functionality of any supporting materials supplied by the authors. Any queries (other than missing material) should be directed to the corresponding author for the article.